AIIM

Association for Information and Image Management
1100 Wayne Avenue, Suite 1100
Silver Spring, Maryland 20910
301/587-8202

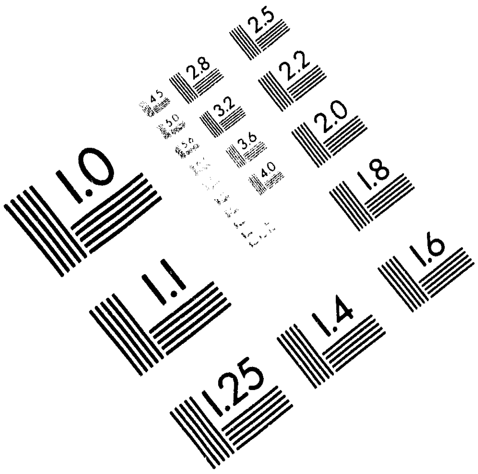

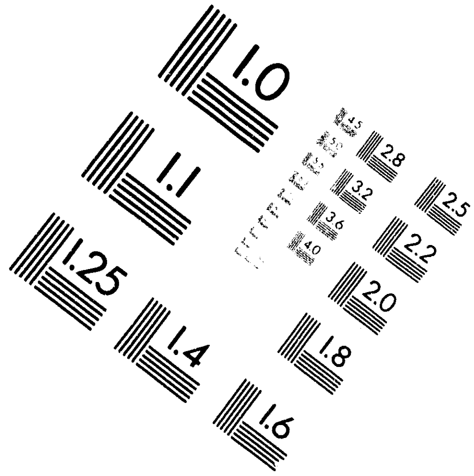

Centimeter

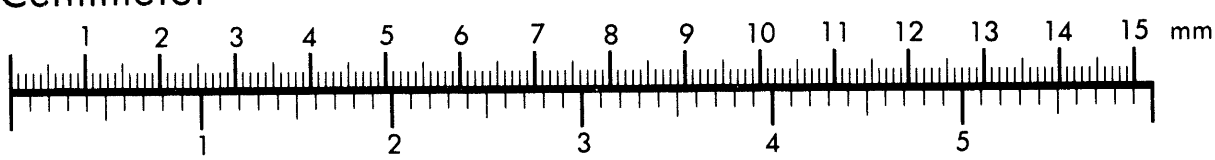

Inches

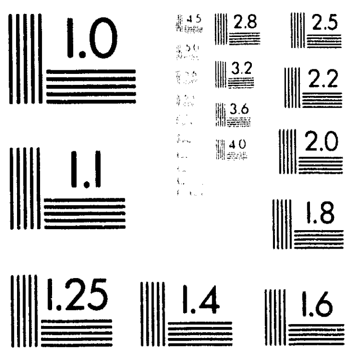

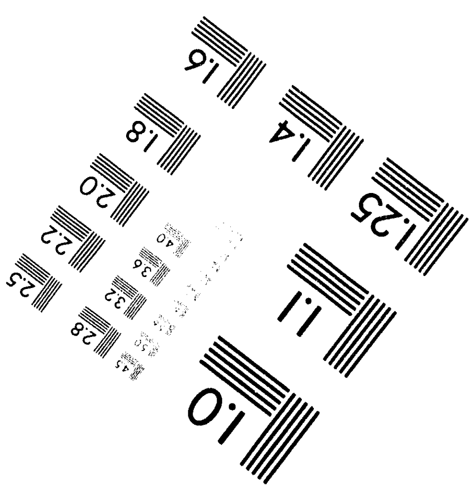

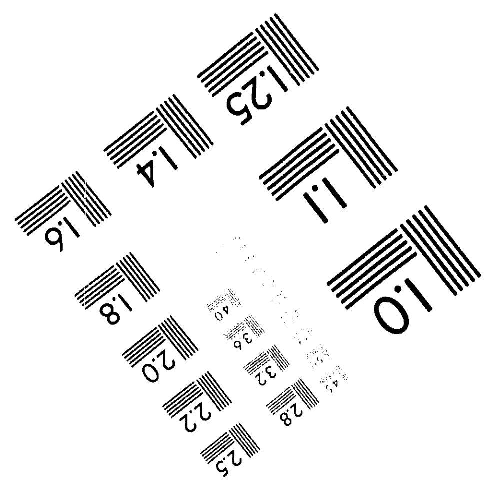

MANUFACTURED TO AIIM STANDARDS
BY APPLIED IMAGE, INC.

1 of 1

ANL/CMT/CP--79802
Conf-931108--38

ANALYTICAL ELECTRON MICROSCOPY EXAMINATION OF SOLID REACTION PRODUCTS IN LONG-TERM TESTS OF SRL 200 WASTE GLASSES

E. C. Buck, J. A. Fortner, J. K. Bates, X. Feng, N. L. Dietz,
C. R. Bradley, and B. S. Tani

ARGONNE NATIONAL LABORATORY
Chemical Technology Division
9700 South Cass Avenue
Argonne, Illinois 60439-4837

Submitted to

Fall 1993 Materials Research Society Meeting
Boston, MA
November 29-December 3, 1993

Work supported by the U.S. Department of Energy, Office of Environmental Restoration and Waste Management, under Contract W-31-109-ENG-38.

ANALYTICAL ELECTRON MICROSCOPY EXAMINATION OF SOLID REACTION PRODUCTS IN LONG-TERM TESTS OF SRL 200 WASTE GLASSES

E. C. Buck, J. A. Fortner, J. K. Bates, X. Feng, N. L. Dietz, C. R. Bradley, and B. S. Tani
Argonne National Laboratory, Argonne, Illinois 60439

ABSTRACT

Alteration phases, found on the leached surfaces and present as colloids in the leachates of 200-based frit (fully active and simulated) nuclear waste glass, reacted under static test conditions, at a surface area to leachate volume ratio of 20,000 m^{-1} for 15 days to 728 days, have been examined by analytical electron microscopy. The compositions of the secondary phases were determined using X-ray energy dispersive spectroscopy and electron energy loss spectroscopy, and structural analysis was accomplished by electron diffraction. Long-term samples of simulated glass, which had undergone an acceleration of reaction after 182 days, possessed a number of silicate secondary phases, including; smectite (iron silicate and potassium iron alumino-silicate, weeksite (uranium silicate), zeolite (calcium potassium alumino-silicate), tobermorite (calcium silicate), and a pure silica phase. However, uranium silicates and smectite have also been observed in tests, which have not undergone the acceleration of reaction, in both the leachate and leached layer, suggesting that these phases are not responsible for the acceleration of reaction.

INTRODUCTION

A comparison of the behavior of simulated and fully active nuclear waste glasses, reacted under static test conditions, has been published previously [1-3]. Feng et al. (1993), have found that 200 simulated (S) glass, reacted at 20,000 m^{-1}, undergoes an acceleration of reaction between 182 days and 330 days. This coincides with the formation of a zeolite phase, which has been identified as clinoptilolite, and an amorphous silica phase [3].

This paper describes the use of analytical electron microscopy (AEM) to identify secondary phases that have formed during the reaction of 200-type glass. Phases were identified both on the leached layers of glass and as colloidal particles within the leachate. Because high-energy electrons interact strongly with matter, electron beam techniques provide a powerful means of characterizing phases that are less than a micron in diameter. However, the strong interaction can result in beam damage to the sample and loss of structural information. Careful work has been required to overcome this problem so that AEM could be used to identify the secondary phases produced during glass corrosion in these tests.

EXPERIMENTAL

Details of glass preparation and experimental design have been published earlier [4-9]. Powder samples of the 200 glass were reacted at 90°C with simulated EJ-13 groundwater. The glass surface area to leachate volume ratio was 20,000 m^{-1}, and the reactions were run for 15 to 728 days. Electron-transparent thin sections of the reacted glass, suitable for transmission electron microscopy (TEM), were produced by ultramicrotomy [10]. Ultramicrotomy tended to shatter the zeolite phase, but enough was preserved to show the spatial relationships between secondary phases.

Phases were characterized using a JEOL 2000 FXII TEM, operating at 200 kV (occasionally using a liquid nitrogen cold stage). The instrument was equipped for X-ray energy dispersive spectrometry (EDS) and electron energy loss spectrometry (EELS). Electron diffraction data from the secondary phases were compared to X-ray diffraction (XRD) data from the literature, and in some cases from experiment, to assist in identifications. The camera lengths for selected area electron diffraction (SAED) were determined by using a polycrystalline aluminum sample. Experimentally derived k-factors for the TEM were obtained, using the Cliff-Lorimer method, from glass and mineral standards [11].

RESULTS

Simulated Glass (200S)

A number of silicate phases were identified in the 200 glass tests, both in the simulated and radioactive glasses. The dominant phase, as determined by XRD and scanning electron microscopy (SEM) analysis, in the 200S series tests which underwent accelerated reaction, was a potassium alumino-silicate. This phase was extremely electron beam sensitive in the TEM, which made structural analysis by SAED difficult.

Potassium Alumino-Silicate Phases

200S glass reacted for 364 and 728 days revealed a potassium alumino-silicate phase, the electron diffraction and XRD data of which is shown in the table below. The XRD spacings, from the 728 day test, of the zeolite phase matched with phillipsite of the harmotome group, ideally $[K_2(Ca_{0.5}Na)_4 (Al, Si)_{16} O_{32}{\cdot}13H_2O]$, a monoclinic zeolite with **a** = 9.88 Å, **b** = 14.30 Å, **c** = 8.67 Å, and β = 124°, (zeolite structural type S4R) [12] (see Table I). TEM had indicated that the zeolite phase was

TABLE I. d-spacings for Potassium Alumino-Silicate

TEM d-spacing (Å) 364 days	TEM d-spacings (Å) 728 days	XRD d-spacings (Å) 728 days[a,b]	Phillipsite,[b] [12]
		8.2	8.14
	6.9 - 7.29	**7.2**	**7.18**
5.67		5.62	
5.20	5.23	5.37	5.38
	4.82	5.0	5.07
	4.72	4.56	
4.25	4.23	4.30	4.30
3.91	4.18	4.12	4.12
3.79		3.73	3.69
		3.57	3.48
3.35	3.33- 3.36	3.5	
3.29		3.26	3.28
	3.23	**3.18**	**3.21**
3.03		2.93	2.93
		2.75	**2.75**
2.56	2.65	**2.69**	**2.69**
2.41	2.35	2.40	

[a]XRD obtained using the Debye-Scherrer method.
[b]Figures in bold are high-intensity reflections.

clinoptilolite in the 364-day test and XRD data suggested that this phase might also be present. X-ray energy dispersive spectroscopy (EDS) showed a high Al/Si ratio, and that both Ca and K were present (see Table II). In the 728-day test, the potassium concentration appeared to be higher, and the phase was, at times, considerably more beam-stable.

Figure 1 shows the interface between the smectite clay and the zeolite phase (the zeolite phase became amorphous while the micrograph was taken, which is why it has the appearance of glass).

The mineral paragenesis during borosilicate glass reaction, in vapor conditions, has been shown by Wronkiewicz [13] to be the following:

unaltered glass ⇒ **smectite clays** ⇒ Na chabazite ⇒ analcime + **phillipsite** ⇒ K-feldspar

The alteration of 200 glass appears to be following a similar paragenic sequence; however, tc date, analcime has not be identified in any of the 200 tests. Chabazite has been tentatively identified in the leached layers of 202U glass reacted at 20,000 m^{-1} for >300 days [14].

Uranium Silicate Phases

Uranium silicate phases were observed in accelerated 200 S glass, but results from other tests, which will be described later, suggest that this phase is not responsible for the observed acceleration. In Fig. 2, a uranium-bearing phase can be seen attached to the clay phases of the corroded layer. The uranium silicates were most often elongated crystallites which are identified as weeksite.

Table III also demonstrates the kind of precision that can be achieved with SAED data for identifying, in this case, a uranium silicate phase.

Calcium Silicate Phases

A calcium silicate phase, consisting of wispy long needles, similar to smectite clay but much straighter, was found in many regions of the leached surface (see Fig. 3). Electron diffraction was obtained from this phase but was weak (see Table IV). Quantitative analysis by EDS suggests $Ca_2Si_7O_x$. Wollastonite is a possible match, but it is a high temperature phase. Other possibilities might be calcium-boron containing feldspar, however solution data, as well as EELS analysis of this phase, suggests that boron is not incorporated into secondary phases. The best match with SAED data was found with orthorhombic tobermorite [$Ca_5(OH)_2Si_6O_{16}.4H_2O$], but a reasonable match was also made with synthetic triclinic gyrolite [$Ca_8Si_{12}O_{30}(OH)_4.7H_2O$], which matched, in terms of composition, closer than the tobermorite. A Si-K EELS absorption edge from the phase has been Fourier transformed to reveal the radial distribution function (RDF) which shows the nearest neighbor distances for silicon (i.e., Si-O bond lengths) (see Fig. 3d).

The tobermorite identified, does not appear to possess enough calcium, suggesting that there is a large amount of silica between the crystallites. Tobermorite and gyrolite are common reaction products associated with the acceleration of glass reaction in vapor conditions [15].

Iron Silicate Phases

A silica-rich phase has been described previously [3], although the phase was rare. More commonly, an iron silicate phase was found that displayed polycrystalline electron diffraction typical of a smectite clay.

TABLE II. Composition* of Zeolite Phases Found in 200S Glass Tests. Zeolites were not homogeneous with respect to K and Ca. Si and Al errors <10%; K and Ca error >50%

	At %			
	Si	Al	K	Ca
364 Days	65.9	25.5	5.1	3.0
728 Days	59.2	28.95	9.15	2.75

*It is not possible to quantify oxygen by EDS due to self-absorption of low energy O-K X-ray and low fluoresence yield (ω_K).

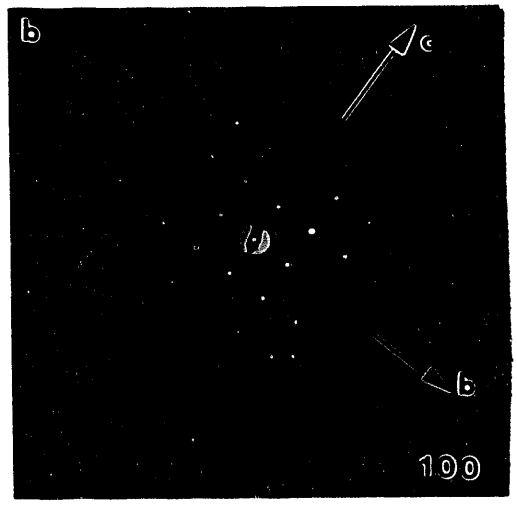

Figure 1. Micrograph (a) of clay and zeolite phases found in 200S glass reacted for 364 days. The zeolite has become amorphous due to the electron beam. (b) Electron diffraction along a major zone axis in zeolite phase from a 728-day test.

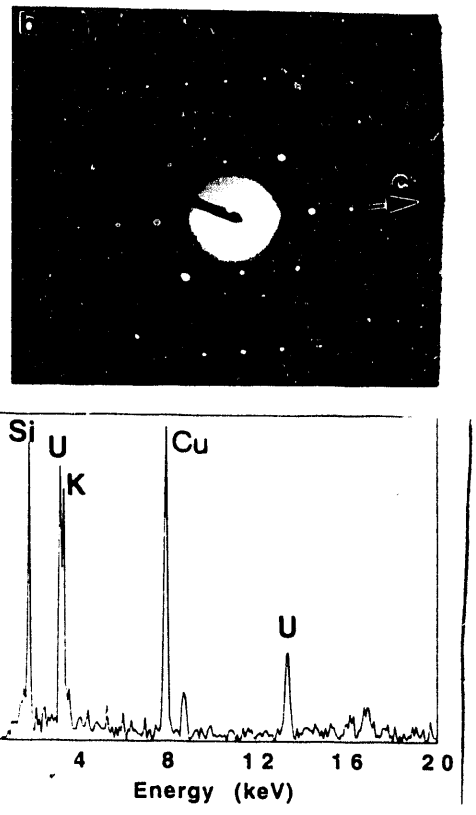

Figure 2. (a) Micrograph of uranium silicate particle attached to clay layer of a 200S glass reacted for 728 days, (b) electron diffraction taken along a minor axis, and (c) EDS compositional analysis (Cu-$K_{\alpha,\beta}$ fluorescence due to support grid).

TABLE III. d-spacings for Uranium Silicate

d spacings (Å) 364 days	d spacings (Å) 728 days	Error ± (Å)[a]	Weeksite[b] [18]
9.07	9.09	0.25	8.98
7.08	7.09	0.16	**7.11**
5.63	6.01	0.11	**5.57**
4.53	4.60	0.08	4.58
	3.69	0.07	----
3.56	3.55	0.06	**3.55**
3.26	3.32	0.05	**3.20 - 3.30**
3.03	3.07	0.05	3.06
2.79		0.04	2.80
2.44	2.51	0.04	2.41
	2.39	0.04	**2.37**
2.29	2.30	0.03	2.28
	1.98	0.02	1.97

[a]Errors based on microscope aberrations and experimental accuracy of measurements.

[b]Figures in bold are high-intensity reflections.

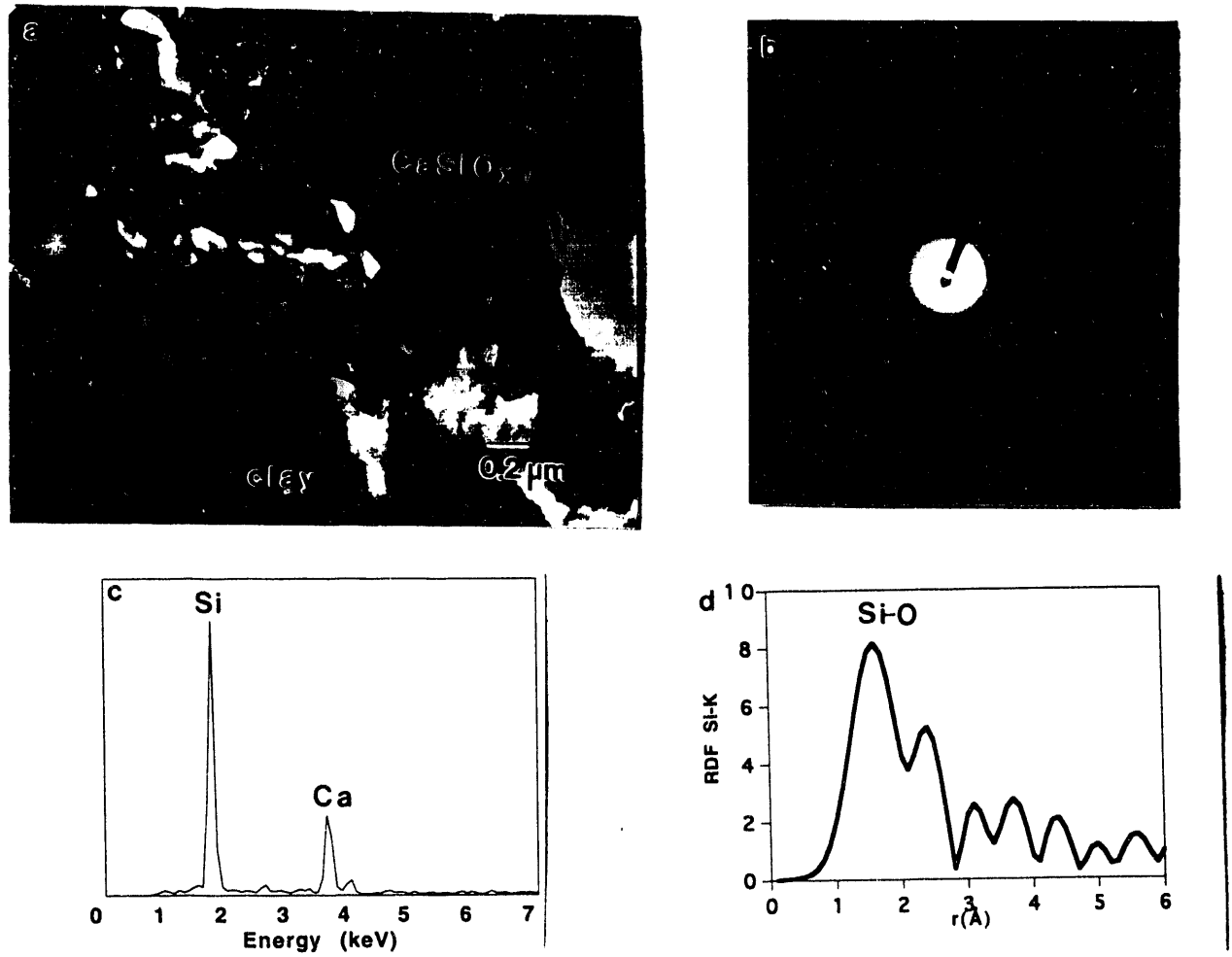

Figure 3. Analysis of a calcium silicate phase found in 200S glass. (a) Micrograph of phase attached to clay layer, (b) polycrystalline electron diffraction pattern, (c) EDS analysis using Be-window detector, and (d) RDF of the Si-K edge, showing Si-O bond length at ~16 Å.

TABLE IV. d-spacings for Calcium Silicate

d spacings (Å)	Error ± (Å)[a]	Tobermorite[b,c]	d spacings (Å)	Error ± (Å)[a]	Tobermorite[b,c]
5.51	0.11	5.49	2.15	0.03	2.15
4.59	0.08		2.03	0.03	2.00
3.57	0.06	3.55	1.86	0.03	1.87
3.15	0.05	**3.16**	1.69	0.02	1.84
3.04	0.05	**3.09**	1.54	0.02	1.54
2.97	0.04	3.005	1.43	0.02	1.44
2.81	0.04	**2.83**			

[a]Errors based on instrument instabilities.
[b]Figures in bold are high-intensity reflections.
[c]JCPDS card 19-1364.

The diffraction pattern in Fig. 4 shows the hk0 reflections of a smectite. The clay was found within the alteration layer, underneath the backbone structure, which is often found in reacted glasses.

Radioactive Glass (200R)

200R glass has not been shown to undergo acceleration by 728 days, so a direct comparison between the two tests can not, as yet, be made. However, a number of secondary silicate phases have been observed in these tests in the leachate from the 200R glass, even though the reaction did not accelerate. The 200R glasses displayed a smectite clay layer, which was depleted of potassium and sodium. This outer clay layer was found to be around 100-150 nm thick at 364 days and 200 nm thick at 546 days, with no evidence of an accelerated reaction.

Colloidal and Suspended Material

The development of colloids in the 200 series of tests will be treated in more detail in a future paper [16]. Smectite clay, identified by its oblique textured electron diffraction pattern [17], was found in the leachate from 200S tests reacted at 20,000 m^{-1} up to 180 days; after this period no colloidal material was found by TEM. In contrast, leachate from 200R glass tests contained potassium-rich clay colloidal material at 364 days, as well as uranium silicate particles (see Fig. 5). In fact, uranium silicate phases have been observed in the leached layers and in the leachate as colloidal particles, in lower SA/V experiments with 200S glass, which have not undergone acceleration. These observations suggest that uranium silicates and smectite clay phases do not cause the acceleration of reaction.

DISCUSSION

Comparison of the 200R glass and the nonradioactive 200S glass, in terms of solution analysis and TEM layer analysis, has been reported elsewhere [2,3]. The zeolite phase, which becomes prevalent during the observed acceleration in reaction, has undergone slight changes between 364 and 728 days, which have resulted in a more beam-stable phase. Uranium silicate (weeksite) phases which were observed in 200S glass reacted at 340 m^{-1} (both in leachate and on the leached layer) and in 200R glass reacted at 20,000 m^{-1} (in leachate) suggests that weeksite is not responsible for the accelerated reaction. The composition of the zeolite phase varies, with some phases possessing a higher potassium content. We have not observed evidence of the formation of feldspar, although the zeolite phases in the 728-day sample do appear to be more stable, with increasing potassium content and lower aluminum content.

We have found that, despite the electron beam sensitivity of many of the secondary phases, good structural analysis by SAED can be obtained. The electron irradiation effects do impede detailed characterization of these phases; as a result, fine structures (such as extended defects and twins) that are common to mineral phases and that may provide further insight into how these phases are forming), cannot be observed; and the electron beam technique is unable to obtain much more information than the more conventional methods such as XRD. Often the data collected, through diffraction and EDS, do not match exactly with the mineral data base. However, as many of the phases exhibit solid solution sequences, small variations in composition and structure can be expected.

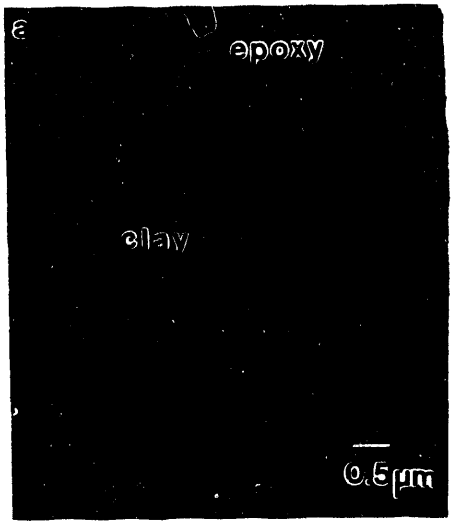

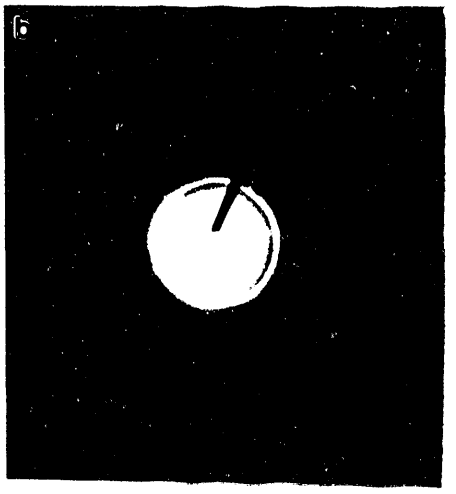

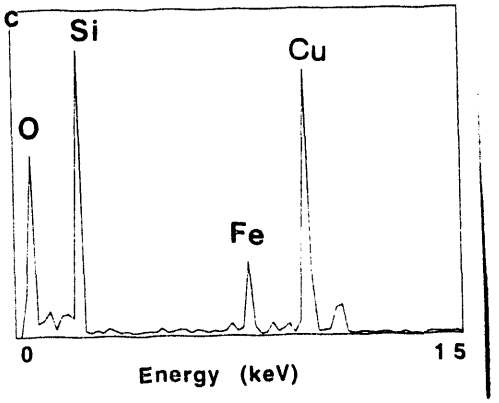

Figure 4. (a) Micrograph of iron silicate phase in a 330-day test, with a diffraction pattern (b) typical of a smectite clay, and (c) EDS analysis of the phase.

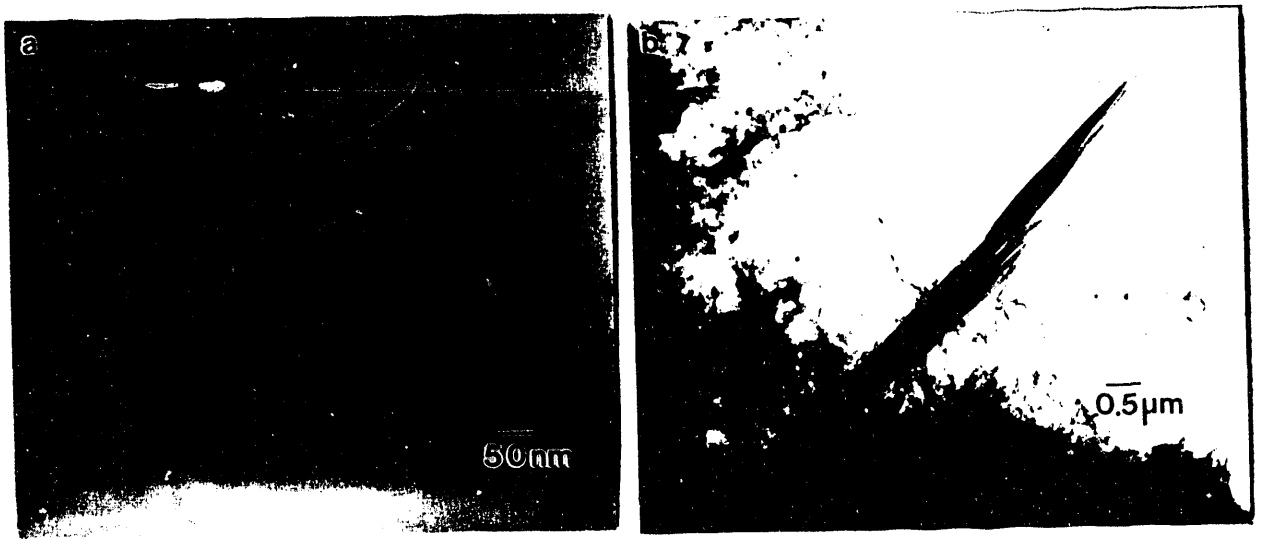

Figure 5. (a) TEM image of clay colloids collected on a "holey" carbon film and (b) uranium silicate particle in 200R leachate reacted for 546 days at 20,000 m^{-1}.

The integration times required to collect EELS analysis of uninterrupted K edges, mostly results in amorphization of the studied alteration phase. However, the bond lengths of covalent phases are unlikely to change during amorphization, (unless there are redox modifications), and therefore radial distribution functions, obtained from the extended fine structure, will still provide information on nearest neighbor distances, so providing some structural data [19].

ACKNOWLEDGMENTS

This work is supported by the U.S. Department of Energy, Office of Environmental Restoration and Waste Management, under contract W-31-109-ENG-38.

REFERENCES

1. J. K. Bates, X. Feng, C. R. Bradley, and E. C. Buck, Waste Mgmt. '92, 1047 (1992).
2. X. Feng, J. K. Bates, C. R. Bradley, and E. C. Buck, Mat. Res. Soc. Symp. Proc. 298, 207 (1993).
3. X. Feng, J. K. Bates, E. C. Buck, C. R. Bradley, and M. Gong, Nucl. Technol. 104, 193-206 (1993).
4. X. Feng and J. K. Bates, Proc. 3rd Inter. Conf. High Level Rad. Waste Mgmt., 925 (1992).
5. J. K. Bates, High Level Radioactive Waste Management, Proc. 2nd Ann. Inter. Conf., Vol. 1, 700 (1991).
6. A. R. Hall, A. Hough, and J. A. C. Marples, DOE/RW/89/115; AERE-R-13071 (1988).
7. L. Werme, I. K. Bjomer, G. Bart, H. U. Zwicky, B. Grambow, W. Lutze, R. C. Ewing, and C. Magrabi, J. Mater. Res. 5, 1130 (1990).
8. J. A. C. Marples, N. Gordon, F. Lanza, and P. van Iseghem, Rad. Waste Mgmt. and Disposal, 287 (1991).
9. N. E. Bibler, Adv. Ceram. 20, 619 (1986).
10. J. P. Bradley and J. K. Bates, Proc. 12th Int. Congress for Electron Microscopy, Seattle, WA, San Francisco Press, pp. 444-445 (1990).
11. G. Cliff and Lorimer, J. Microscopy (1975).
12. G. Gottardi and E. Galli, Natural Zeolites, p 326, Springer-Verlag, Berlin (1985).
13. D. J. Wronkiewicz, J. K. Bates, T. J. Gerding, E. Veleckis, and B. S. Tani, J. Nucl. Mater. 190, 107-127 (1992).
14. E. C. Buck, unpublished results.
15. J. K. Bates, L. J. Jardine, and M. J. Steindler, Science 218, 51-54 (1982).
16. E. C. Buck, J. K. Bates, and X. Feng, submitted to American Ceramic Society Annual Meeting, Indianapolis, IN (April, 1994).
17. E. C. Buck, J. K. Bates, J. C. Cunnane, W. L. Ebert, X. Feng, and D. J. Wronkiewicz, Mat. Res. Soc. Symp. Proc. 294, 199-206 (1993).
18. W. F. Outerbridge, M. H. Staatz, R. Meyrowitz, and A. M. Pommer, Am. Miner. 45, 39-52 (1960).
19. J. Fortner, E. C. Buck, and J. K. Bates, Bull. Am. Phys. Soc. (March 1994).

DATE FILMED

6/24/94

END